ISSN 1070-3632, Russian Journal of General Chemistry, 2015, Vol. 85, No. 5, pp. 1270–1283. © Pleiades Publishing, Ltd., 2015.
Original Russian Text © A.S. Ivanov, A.F. Pal, A.N. Ryabinkin, A.O. Serov, E.A. Ekimov, A.V. Smirnov, A.N. Starostin, 2013, published in Rossiiskii Khimicheskii Zhurnal, 2013, Vol. 57, Nos. 3–4, pp. 70–82.

Application of Dusty Plasma for Production of Disperse Composite Materials

A. S. Ivanov[a], A. F. Pal[b], A. N. Ryabinkin[b], A. O. Serov[b], E. A. Ekimov[c], A. V. Smirnov[d], and A. N. Starostin[e]

[a] *National Research Centre "Kurchatov Institute," Akademika Kurchatova pl. 1, Moscow, 123182 Russia*
e-mail: asi.kiae@gmail.com
[b] *Skobeltsyn Institute of Nuclear Physics, Lomonosov Moscow State University, GSP-1, Moscow, 119991 Russia*
e-mail: aserov@mics.msu.ru
[c] *Vereshchagin Institute for High Pressure Physics (HPPI RAS), Russian Academy of Sciences, Kaluzhskoe shosse, str. 14, Troitsk, Moscow, 142190 Russia*
[d] *Lomonosov Moscow State University, Faculty of Chemistry, GSP-1, Moscow, 119991 Russia*
[e] *Troitsk Institute of Innovative and Fusion Research State Research Center of the Russian Federation (TRINITI RSC RF), ul. Pushkovykh, vladenie 12, Troitsk, Moscow, 142190 Russia*

Received January 1, 2013

Abstract—Objectives and achievements of the production of disperse composite materials (DCMs) which consist of particles with a metal coating are represented. The prospects of the DCM production by the dusty plasma method based on confining a cloud of micron-sized particles in a discharge plasma and on magnetron sputtering are shown. The method was tested in the preparation of catalyst materials, a superhard diamond polycrystalline material, and a polyquasicrystalline material with a low friction coefficient. The results of investigations of the structure and properties of powdered and sintered DCMs are presented.

DOI: 10.1134/S1070363215050448

INTRODUCTION

The progress in the development of novel composite materials is associated with the possibility of production of materials with unique physicochemical properties in response to demands of fast progressing fields of science and technics, including medicine, space industry, transport, etc. A composite material should combine the properties of its structural components so that to ensure enhanced strength, plasticity, durability, and friction coefficient. The most part of composite materials comprise structural components of a plastic matrix and inclusions of the second phase as powders or fibers [1]. Among them, metal matrix composites reinforced by a ceramic filler can function in extreme operating conditions. There are two technologies of production of such materials: mixing metal powders and ceramics followed by fusion and infiltration of a liquid metal into a porous template. Certain technological processes, for example, catalysis, require metal ceramic composites containing no metal matrix. Such materials are fabricated by metal vapor deposition on refractory and chemically stable ceramics or on a fiborous or layered carrier [1].

Composite materials with the particle sizes varying from fractions to hundreds of micrometers may be referred as disperse composite materials (DCMs). For example, the particle size in the polycrystalline diamond materials for use in high-precision cutting tools should be close to the lower boundary of the mentioned range, and the metal content should be no higher than a few percent [2]. By mixing powders (diamond and a binder) one cannot achieve homogeneous distribution of reactants, especially if the particles to be sintered are smaller than 5 μm [3, 4]. Metal infiltration to a diamond powder also has disadvantage for production of diamond composites in view of the inhomogeneity of structural and mechanical characteristics, which develops along the infiltration direction [5]. As the diamond particle size decreases, the infiltration depth radically decreases [6] because of diamond graphitization and filling of pores with a nondiamond carbon. By contrast, metal vapor deposition on diamond particles

allows one not only to control the concentration of the binder, but also to provide its uniform distribution in the bulk of the sintered diamond materials.

Performance characteristics of metal–ceramics composites, including DCMs, are strongly affected by interphase interaction between their structural components. Thus, by coatings the reinforcing particles with special materials one can significantly enhance adhesion between structural components of matrix composite materials [7]. Such coatings can be applied by traditional methods (sol–gel process [8], electrochemical deposition [9], electroless method [10–13], chemical vapor deposition (CVD) [14–18] and its version with the use of gas-discharge plasma [19, 20]. Along with chemical methods, efficiency of physical vapor deposition (PVD) has been proved.

Magnetron Sputter Deposition of Coatings

Physical vapor deposition of coatings is most commonly performed in gas discharge plasma. The advantage of plasma-enhanced deposition is that the surface being treated is activated by energetic species of the charged component of the plasma, while the temperature of the neutral component remains fairly low. The mean energy of the species (atoms or ions) of the component being deposited in a plasma deposition process may vary over a wide range and is usually much higher than in a CVD process. To form defects that would act as surface activation centers, energies of about a few electron volts are required [21]. Energies of several hundred electron volts may prove sufficient for particles to be deposited to penetrate into the surface layer of the substrate and give rise to sputtering, radiation-induced diffusion, and cascade mixing processes [22]. Therewith, a transition layer comprising coating and substrate particles is formed. Together these processes favor, to a greater or lesser degree, enhanced adhesion of the coating [23]. The stronger is adhesion, the lower is surface migration of deposited metal particles at elevated temperatures and, consequently, the higher is the operating temperature and the durability of the resulting materials, for example, catalyst [24, 25].

The energy of sputtered particles coming to the surface being treated also strongly affects the structure of the growing film [26]. Fast atoms additionally heat the surface and activate migration of absorbed coating atoms. This accelerates crystallite growth in a direction perpendicular to the incident flux direction and formation of larger crystals.

Several works showed advantages of magnetron sputter deposition of metal coatings over chemical methods. Magnetron sputter deposition provides more uniform coatings [10] and allows control of film structure on particles [27]. In magnetron sputtering systems plasma is characteristically located close to the sputtering target, due to which the substrate temperature may be not very high [21]. Magnetron sputtering allows deposition of films of almost all metals, as well as multicomponent coatings with highly precise components contents [28–30], whereas the assortment of metal coatings which can be produced by pyrolysis of organometallic compounds is limited by the fairly narrow range of developed precursors. The applications of magnetron sputtering are not limited by the requirement that the treated particles be dielectric in nature, like is the case in electrochemical methods; for example, metals coatings can be deposited on diamond particles [31–35] and glass spheres [36–38].

A possible practical application of plasma depositions is the production of disperse catalysis. The idea to deposit a catalytic coating on particles with a low specific surface area by means of metal plasma sputtering was advanced by Cairns et al. [39]. This technology excludes contamination of the catalyst and opens up the possibility for controlling the size of the resulting metal particles in the nanometer range [40]. Thus, magnetron sputtering was used to prepare disperse catalysts on the basis of platinum particles 3.5 nm and smaller in size, deposited on different substrates [41–43]. The catalytic material in [44] was obtained by sputtering a gold target.

The morphology of the coatings fabricated by plasma sputtering is much dependent of the process parameters. In a limiting case, the coating is a film, while in another case it consists of individual nanoparticles. In the first case the coating is formed by sputtered atoms adsorbed on the support, in the second, by clusters formed in the gas phase.

A deposition technology that makes use of a dusty plasma (partially ionized gas containing solid particles) [45] allows deposition of coatings on micron-sized particles. In this case the specific surface area of the support is no larger than 10 m^2/g, and to obtain an active catalyst, the dispersity of the catalytic component should be as high as possible. In cases where nucleation of the catalytic material in the gas phase is excluded, its dispersity will be controlled by the nature of the coating and its treatment technology.

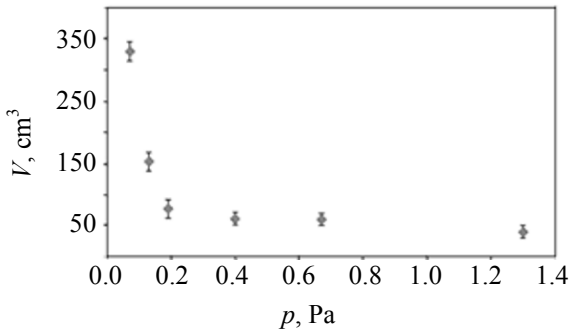

Fig. 1. Dependence of the volume of a dust cloud confined in an RF discharge plasma on the pressure of plasma-forming gas.

Many characteristics of disperse composites are improved as the particle size is decreased and the particle surface area-to-volume ratio is increased. However, smaller particles are more difficult to disperse. Lowe and Hosford [36] found in their work on the RF magnetron sputter deposition of coating on single particles (size 500 μm) that, if the particle to be coated is levitating in the working gas and does not contact with solid surfaces, the resulting surfaces are the most uniform and smooth. Just such process design should be envisioned. Desirably, not one but a lot of particles be present in the levitation state.

Magnetron sputter deposition relates to line-of-site technologies, i.e. it does not suggest any shielding objects between the treated surface and the sputtered material. Mechanical separation of particles from each other with the use of vibrations of different frequencies was applied in [10, 27, 34, 46–48]. Magnetron sputtering allowed uniform coatings to be deposited on 10–100-μm particles, but the results with particles smaller than 10 μm were poor, because the problem of dispersing small particles had not been solved completely.

The widely used fluidized bed technology is efficient with particles no smaller than 50 μm and having a low bulk density [10, 49, 50]. A classical fluidized bed technology is unsuitable at low working gas pressures [49]. One of the ways to enhance the efficiency of this technology is the introduction of gas discharge plasma to the process. Thus, Snyder et al. [51] complemented the process of dispersion of 50-μm particles by the fluidized bed technology by the initiation of an inductive RF discharge in the chamber filled with particles. It was experimentally established that in the presence of plasma the concentration of particles in the bed increases several times.

The use of magnetron sputtering for the deposition of metal coatings on micrometer-sized particles levitated in RF plasma was proposed in [52, 53]. One of the limitations of this version of the process is that the dusty plasma trap, where the levitating dust particles are mixed, has a low volume, which decreases the efficiency of the coating deposition process. Stoffels et al. [53] observed destruction of the particle cloud, when the magnetron sputter was turned on. A conclusion was thus drawn that this approach holds limited promise but later it was further development [31, 32, 45, 54, 55].

The aforesaid allows the following conclusion. Magnetron sputtering is a promising technology for deposition of uniform coatings on disperse particles. The overwhelming majority of presently developed technologies are suitable to deposit coatings on particles no smaller than tens micrometers. One of the ways to increasing dispersity of particles to be treated involves the use of dusty plasma.

The aim of the present work was to make use of the advantages of plasma methods in deposition coatings on particles whose size varies in the range 1–10 μm.

Dusty Plasma Deposition of Coatings on Particles

Particle Cloud Parameters in an RF Plasma Trap [54–61]

In [60] we performed an experimental study of the effect of a dc magnetron discharge on the parameters of the dust cloud formed in RF plasma. The RF discharge was maintained in a metal reactor chamber mounted inside a vacuum chamber. Micrometer-sized monodisperse particles were injected in plasma with an inertial disperser. In the presence of RF plasma in the reactor, the dusty plasma trap retained the injected particles not letting them to deposit to the reactor bottom. As a result, a dust cloud with the volume much dependent on the working gas pressure is formed. Turning-off the RF discharge lead to fast particle deposition.

It was found that the largest microparticle dust clouds are formed at working gas pressures varying from 0.07 to 0.13 Pa (Fig. 1).

This range corresponds to the gas pressure range characteristic of magnetron sputter deposition processes. The large volume of the particle cloud and its long life time, as well as the presence of a characteristic range of plasma-forming gas pressures allowed us to suggest that such particle confinement conditions can be used in a coating deposition process.

To assess the efficiency of the process to be designed, we should determine the concentration of particles in the dust cloud. This concentration can be assessed by the attenuation of light radiation after passing through the dust cloud [62]. As known, the absorption of laser radiation in a cloud of particles depends not only on the concentration but also on the size of the particles. The particle size for the present experiment was chosen on the basis of the following considerations. First, as found in [57], compact particles larger than 16 μm at a mean bulk density of the material of 2 g/cm^3 and higher, are not retained for a long time in a dusty plasma trap, while heavy thread-like agglomerates are retained in a strong electric field at the very bottom of the trap.

Second, undesirable particle agglomeration due to the ballistic overcome of the screened repulsion potential [63] or due to attraction associated with polarization of particles [64, 65] may occur in the plasma. Agglomeration of like-charged particles in the cloud occurs, if the size of these particles is larger than a critical size [65]. According to calculated and experimental results [57], at concentrations of about 10^4 cm^{-3}, which are characteristic of laboratory experiments, the critical size is a few micrometers. This imposes additional restrictions on the upper limit of the size range of particles subject to treatment in a dusty plasma trap: The particles injected to the plasma should be smaller than 10 μm.

Study of the surface of the substrates placed inside the reactor showed that 90 % of adsorbed particles are not aggregated with each other, implying that in the middle part of the cloud there should be particles whose size is close to the mean particle size in the sputtered powder. With this in mind, we can estimate the particle concentration in the middle part of the cloud by the absorption of laser radiation, not measuring the particle size *in situ*. Assuming that the particle size is equal to the mean particle size in the powder (5.4 μm), the particle concentration in the middle part of such cloud, estimated by the Bouguer–Beer formula, is 2×10^4 cm^{-3}. Note that the volume of the steady-state dust cloud at such concentration is 330 cm^3 [60] (Fig. 1).

The plasma parameters characteristic of the RF discharge used in the present work and the measured particle velocities (by particle tracks) allowed estimation of the interaction parameter between charged plasma species by the following formula (including charge screening in plasma) [66]:

$$\Gamma = \frac{q^2}{4\pi\varepsilon_0 klT}\, e^{-l/R},$$

where q is the particle charge; ε_0, electric constant; l, mean particle–particle distance; R, screening radius of a point charge in the plasma; and k, Boltzmann constant.

Assuming that the temperature of the dust components is equal to that of the gas component, we obtain $\Gamma = 80$. The high plasma nonideality parameter suggests that interaction between particles has a strong impact on their dynamics (repulsion at a small particles size) and can explain the absence of particle agglomeration in the dust cloud.

Effect of Different-Type Magnetron Sputter Discharges on the Dust Cloud

To increase the concentration of particles in the dusty plasma trap, one should tend to minimize the effect of magnetron sputter on the characteristics of the RF discharge in the reactor. As known, the spatial distribution of plasma parameters between the sputtered target and the substrate, and, consequently, the effect of the magnetron discharge on the remote substrate, are much dependent on the electron and ion fluxes from the plasma [21], which, in their turn, depend on the configuration of the magnetic field of the sputter.

In our experiments [60] we used magnetic systems of different types: balanced and unbalanced with a strong external pole. As the sputter discharge power was varied in the range 30–300 W, deformation of the dust cloud boundaries was observed, and the cloud shifted inside the discharge chamber. In the case of an unbalanced sputter, the cloud strongly shifted inside the chamber, and a space free of particles formed in the middle part of the chamber. By contrast, turning on the balanced sputter causes reversible motion of the cloud in the discharge chamber and slightly decreases (by 20 %) the particle concentration in the middle of the reactor [60]. In the case of the balanced magnetron, the plasma density and electron temperature are lower, and this explains why the balanced magnetron has a weaker effect on the dust cloud confined in the discharge chamber. In this case, electrons that are higher in energy and have left the cathode trap come to the anode. In the case of the unbalanced magnetic system, electrons are trapped by the magnetic field outside the cathode trap, reach the substrate region and ionize the gas. In the substrate region, secondary plasma is generated [67].

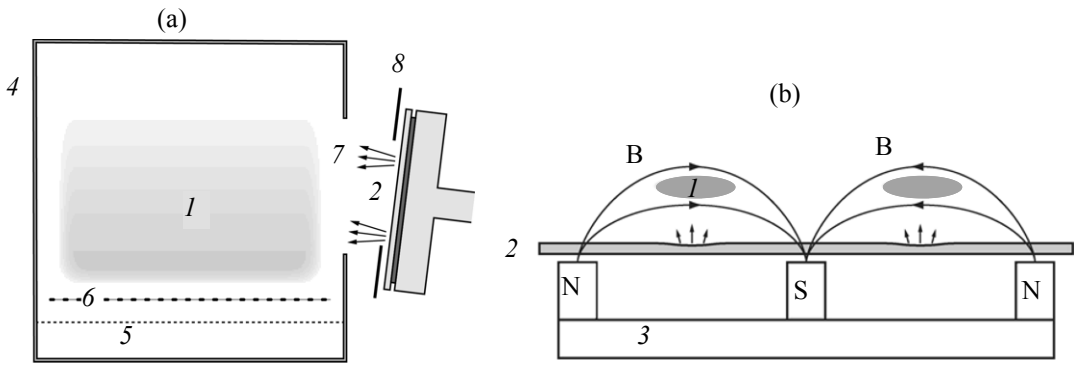

Fig. 2. Alternative systems for dusty plasma deposition of coatings on microparticles: (a) confinement of dust cloud in an RF discharge plasma on metal sputtering outside the RF dusty plasma and (b) confinement of particles and metal sputtering in an RF magnetron discharge plasma: (*1*) dusty plasma cloud; (*2*) sputtering target; (*3*) sputter magnetic system; (*4*) reactor housing; (*5*) disperser; (*6*) loaded RF electrode; (*7*) inlet hole for sputtered atoms; and (*8*) screening electrode.

Let us estimate the performance of the DCM production by magnetron sputter coating of dust cloud particles. Let N_d is the number of dust particles simultaneously retained in the cloud; G, particle coating growth rate; and t, time required to deposit coating with thickness D on N powder particles. The latter two values are related to each other by the formula $D = GN_dt/N$. The usual growth rate of coating on a macrosubstrate at the magnetron power of 0.5–1 kW is a few nanometers per second. It should be borne in mind that the coating growth rate on a 3D particle is several times lower than on a plane substrate. With the measured dust cloud volume of 330 cm^3 and particle concentration in the cloud of 2×10^4 cm^{-3}, we find that within a reasonable experiment time (2 h) a 10-nm coating will be obtained on 5×10^9 particles, i.e., provided the mean size of a spherical particles of 6 μm, about ~1.1 cm^3 of the powder will be treated.

There are a number of factors that make the proposed process scheme difficult to realize. First, to deposit coating of the large surface of small particles with acceptable performance requires that the power of the magnetron sputter be no less than 10^2 W. Second, the fact that the particle concentration in the dust cloud decreases as the sputter power is further increased makes it impossible to increase the mean coating deposition rate. Third, incomplete dispersion, as well as the possibility of particle agglomeration increase the probability of incomplete coating of particles in the resulting DCM. Fourth, increasing agglomeration rate does not allow the concentration of dust particles to be increased considerably.

Taking account of the above factors, we considered rational a cyclic process design, where the particles being treated are periodically returned to the dispersion system. Furthermore, in view of the enhanced requirements to the dispersion system, one should ensure that the powder is separated into fragments whose size does not exceed the critical coagulation radius.

Deposition of Coatings in a Reactor with the Sputtering Target Separated from Particle Cloud

Figure 2a presents one of the versions of the dusty plasma deposition of coatings on microparticles of a powder dispersed outside the plasma zone. The microparticle cloud is formed in an RF discharge which is maintained inside the reactor. A flux of atoms from the magnetron sputtering target is directed to nonlevitating particles that are continuously fed to the cloud from a disperser through a mesh loaded electrode located in the bottom part of the reactor.

The disperser is separated from the discharge chamber with a mesh upper partition. The disperser–loaded electrode distance is a few millimeters. Such design allows particles to circulate between the cloud and disperser. Before start of operation, the disperser is loaded with dispersing elements and a powder comprising micron-sized particles. On exposure to mechanical vibrations (frequency 50 Hz, amplitude 1.5 mm) the powder particles go to the discharge chamber. The volume of the dust cloud in the chamber may reach 1.2 dm^3 in presence of RF discharge.

For coating particles in the cloud, metal atoms can be injected in the reactor through a hole in the reactor sidewall so that the sputtered atoms get directly into the dust cloud, whereas the disperser and RF electrode are beyond visual line of sight from any sputtering

track point or can be injected from above. The first variant is preferred, because in this case coating is deposited exclusively on particles levitating in the plasma. To test the developed technology, we performed the following experiments:

– sputter deposition of a catalytically active element on aluminum, silicon, and zirconium oxide particles;

– sputter deposition of cobalt on diamond powder particles to obtain a uniform fine diamond charge with a minor activating additive for production of a superhard material;

– sputter deposition of nickel and copper on a quasi-crystal powder particles for production of a material having enhanced strength and a low friction coefficient.

Adaptation of the Technology for Production of Catalytic Coatings

Before passing to discussion of the resulting experimental data, we would like to give some explanations.

A film coating is formed from target atoms that are adsorbed on the surface of a substrate; however, under certain conditions, sputtered atoms being in gas can form particles that deposit on the surface. According to the model in [68], homogeneous nucleation of two-atomic molecules and film growth initiation involve thermalized sputtered atoms (the retardation stage). Normally, the energy loss of an atom due to collisions with buffer gas atoms is characterized by a parameter pd (p is the pressure of the buffer gas and d, distance from an observation point to a sputtered point). The distance from the sputtered target to the site where an atom released from the target with a mean energy becomes a thermal atom is defined as the thermalization length d_{th}. Particles formed in the gas phase can deposit on the substrate if the latter is separated from the target by a distance larger than d_{th}. Based on the results of deposition of palladium coating of different morphologies [40], calculations and measurements of d_{th} [69, 70], taking account of the effect of substrate on the energy distribution of sputtered atoms [71], and taking d to be equal to the distance from the target to the middle part of the cloud we can expect formation in the gas phase, at pd = 1000 Pa mm and a sufficient sputter power, of palladium nanoparticles which will deposit on dust particles. At $pd \leq 100$ Pa mm, film growth takes place on particle surface.

To produce DCMs on the basis of Al_2O_3, SiO_2, and ZrO_2 with a catalytic coating containing Pd clusters, we used Al–Pd and Zr–Pd plane mosaic sputtering targets. The target size was increased, which allowed coatings to be deposited at a buffer gas pressure 30 times lower than in previous experiments [45].

Two groups of experiments were performed. The first group of experiments involved deposition of Al–Pd coatings on silicon plates located at distances d (30–400 mm) from the target. Coatings both on the substrate sides looking to the target and on the reverse sides of the substrates were obtained. The second group of experiments involved production of DCMs on the basis of an Al_2O_3 powder with an Al–Pd coating and on the basis of a ZrO_2 powder with a Zr–Pd coating. No palladium was detected on the reverse sides of substrates whose position corresponds to $pd < 25$ Pa mm, which suggests that the thermalization region which serves as a source of palladium diffusion to the reverse side of the substrate is at much higher pd values.

The resulting data allowed us to determine the order and conditions for deposition of Pd-containing coatings on powder particles. The following conditions were established for film coatings: working gas pressure 0.17 Pa, distance from the middle of the reactor to the magnetron 200 mm. The size of Al_2O_3 particles with an Al–Pd coating is 5–10 μm, and the size of ZrO_2 particles with a Zr–Pd coating is 0.2–10 μm. The Pd contents in the coatings varied from 0.2 to 2 wt %.

The main component of the coatings is an Al_6Pd phase (Fig. 3); in addition, metallic aluminum and its oxide are present. In the coating on the Zr-Pd/ZrO_2 particles, zirconium is oxidized almost completely.

Deposition of Coatings on Particles in an RF Magnetron Discharge Plasma

The above-described coating technology does not allow one to treat brittle particles. Figure 2b shows a version of sputter film deposition on such particles [55], but here, unlike what is shown in Fig. 2b, particles are confined in a capacitive RF magnetron discharge plasma in a ring-shaped trap, and the same discharge was used to sputter the target electrode.

Magnetron discharges relate to anomalous discharges, i.e. the discharge current density can be higher than normal, but, unlike discharge in the absence of magnetic field, this discharge occupies a small part of the target electrode surface. The potential distribution in a magnetron discharge plasma [72, 73] and corresponding electric field lines [74] ensure

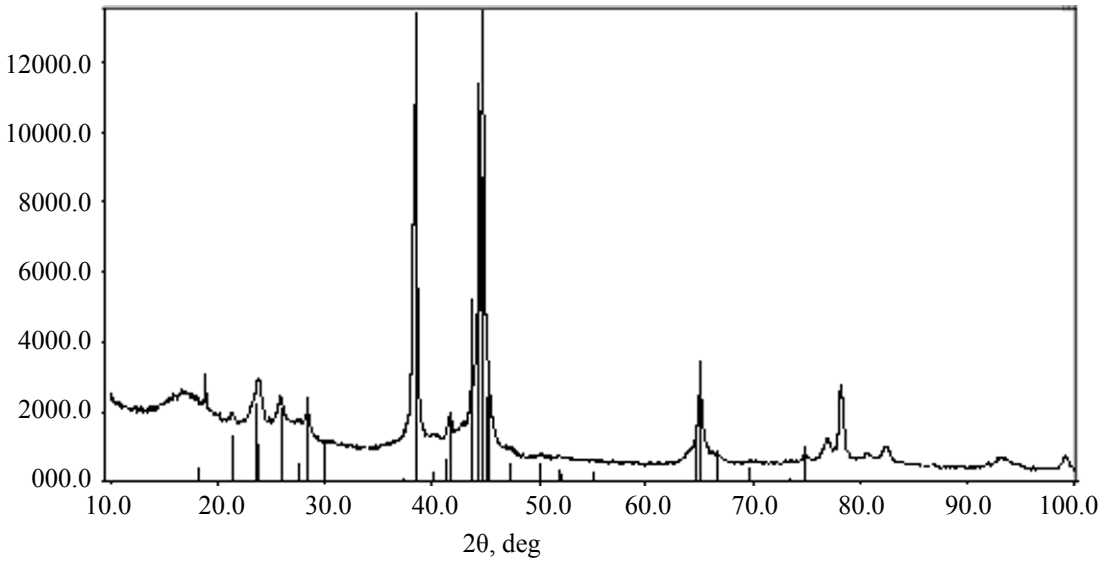

Fig. 3. X-ray diffraction patterns of the Pd + Al film obtained by magnetron sputtering on a plane plate at a pressure of 0.17 Pa. Shown are the reflexes of the Al_6Pd phase.

formation of an electrostatic trap for particles in such plasma, even if the electrode does not have macroscopic deviations from a plane shape. Plasma electrons move along magnetic field lines (see Fig. 2b) to a weaker magnetic field region, where the plasma density and its potential increase forming a trap for particles. The most efficient ion bombardment of the electrode takes place under this region. The electrode surface is sputtered to form a beam of atoms which form coating on particles in the trap.

In [55], powders comprising 0.4–12-, 8–26-, and 15–32-μm glassy carbon balls (Hochtemperatur-Werkstoffe, Germany), 5.4-μm monodisperse silica particles (microParticles, Germany), or 15–100-μm glass spheres were injected in plasma. The particles were injected by a nondestructive technique involving additional electrostatic charging of particles adhered to the electrode [75]. This dispersion technique allows an almost complete separation of particles from each other without damaging them. The treated particles are confined very close to the target electrode (at a distance of 1–3 mm, depending on the particle mass, magnetic induction in the plasma region, gas pressure, and discharge power), within the region of ballistic bombardment with sputtered atoms ($pd < 40$ Pa mm).

All the particles had a uniform coating after treatment (Fig. 4). The roughness of coatings on most spheres in the case of a copper sputtered target (Fig. 4d) is much smaller than in the case of silver coatings (Fig. 4b), and they have a metallic luster and a characteristic reddish yellow color [55]. The mean film growth rate is about 0.1 nm/s.

In the described sputter deposition system, particles move by trajectories along the closed contour of the trap [76] in the direction of the circulating electron current in the magnetron [77]. Such motion ensures the same conditions of sputter deposition on particles of the same size and mass and, consequently, the same coating parameters on such particles.

As known, the film structure is determined by the densities of the ion and neutral atom fluxes to the support surface, radiation flux density, and heats of surface condensation and recombination processes [21]. These parameters depend on the *pd* parameter. Particles with a great difference in mass and size are present in the plasma at different distances *d* from the target, and this leads to visible differences in film structure: from coarse crystals to dense films with a columnar structure (see Figs. 4c and 4d).

Note that the relationships between the above parameters much differ from those characteristic of sputter deposition on larger substrates. The distance *d* between the target and substrate particles is smaller by 1–2 orders of magnitude, and, therefore, their heat exchange takes force in this case [78]. The relationship between the current densities of sputtered metal atoms and buffer gas atoms reflected from the target change significantly (because the initial angular velocity

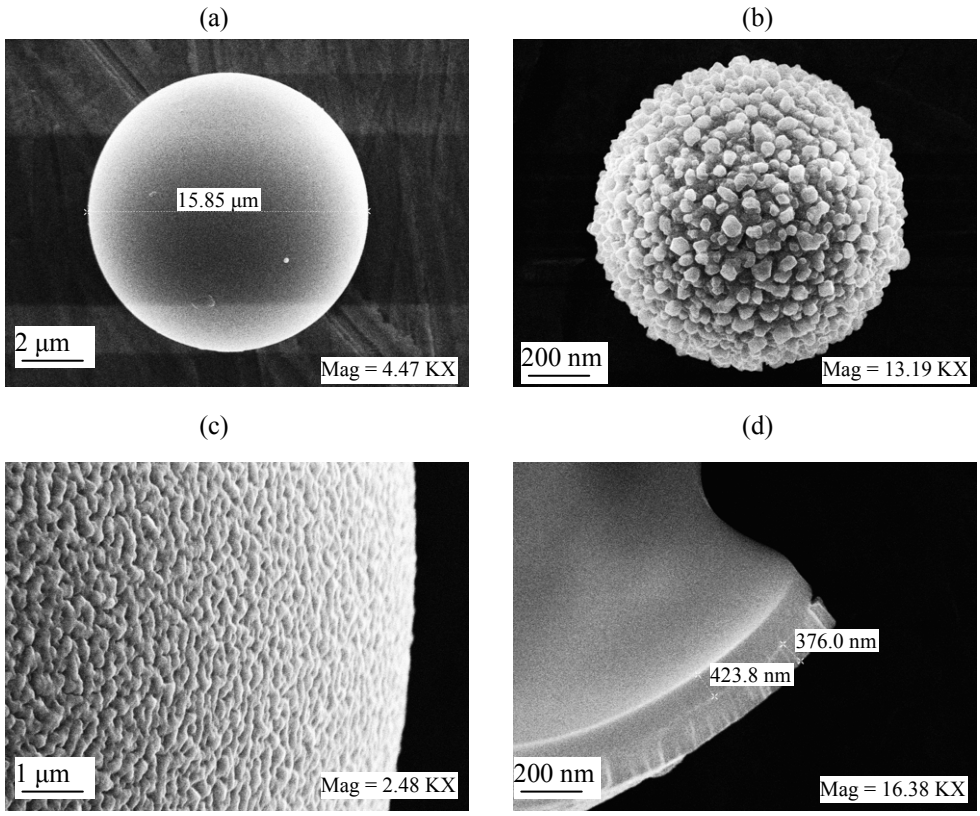

Fig. 4. Scanning electron microscopy images of particles: (a) surface of the initial glass sphere; (b, c) particles with silver coatings of different morphologies; and (d) fracture of a copper-coated sphere.

distributions of these atoms much differ from each other [79]); furthermore, the energy of ions bombarding substrate particles is affected by the electric field at the outer edge of the ion layer [80]. To study coatings deposited at unusual relationships between process parameters may be of independent scientific interest.

Methodical Aspects of the Production of Disperse Composite Materials

Catalytic Systems

To determine the temperature of thermal decomposition of Al–Pd in the initial Al–Pd films, we subjected powders and films to thermal treatment at varied temperatures. The X-ray diffraction patterns of the films show that palladium aluminide decomposes to a considerable extent only in the films annealed at temperatures higher than 750°C. As the annealing temperature is increased, the oxygen concentration in the films increases compared to the initial film [up to 30 times in the film annealed at 770°C, according to EDX analysis data]. Simultaneously the aluminum content decreases, implying that increasing annealing temperature increases the content of alumina in the films. The surface of annealed films contains contrast fields enriched with palladium (backscattered electron and EDX analyses in SEM). The resulting data are consistent with the results in Gurrappa and Wilson

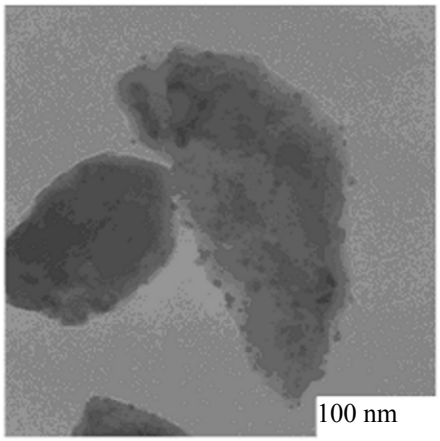

Fig. 5. Images of coated corundum particles (0.4 % Pd/Al_2O_3 powder). Transmission electron microscopy.

Catalytic activity of the Pd/Al_2O_3 and Pd/ZrO_2 systems in the hydrogen oxidation reaction

No.	Sample composition and annealing temperature	S_{sp}, m^2/g	Initiation of the reaction without external heating at $C(H_2) = 4\%$	Self-sustained hydrogen conversion (%) at the H_2 concentration				Hydrogen conversion with external cooling to room temperature, %, at $C(H_2) = 4\%$
				4%	3%	2%	1%	
1	0.6 at % Pd/Al_2O_3	2.5	–	94	97	0	0	0
2	0.6 at % Pd/Al_2O_3	2.5	–	95	95	0[a]	0	0[a]
3	0.6 at % Pd/Al_2O_3	2.5	+	98	96	89	11	70
4	0.2 at % Pd/ZrO_2	4.1	+	100	98	79	36	99
5K	1.5 at % Pd/γ-Al_2O_3	143	–	100	100	75	0[a]	98

[a] In 5 min after flow reduction.

[81], who observed palladium aluminide decomposition and palladium diffusion to film surface at 800°C. To obtain catalysts on the basis of disperse composites, the starting samples containing palladium aluminide were annealed in air at 650, 870, and 1000°C.

The activity of palladium in oxidation reactions is known to be strongly affected by its reaction with the substrate, and the strongest effect is observed in a Pd/ZrO_2 system [82]. The smaller the grain, the stronger is this effect. Therefore, the interaction with the substrate stabilizes palladium oxide more strongly on the smallest metal grains, whereas more active centers are on larger grains. By contrast to that, the resulting catalyst activity is the higher, the larger is the specific surface area of the active element, which decreases with increasing grain size.[1] Since the palladium grain size in the material produced in plasma is below 12 nm, and zirconium was oxidized almost completely, no annealing was performed in this case.

Before catalytic tests the obtained powdered composite materials were compacted at the pressure 3 GPa and temperature 450–500°C for 20 s by the procedure in [83], after which the compact was crushed, and the fraction 0.25–0.5 mm was sieved out.

[1] The regime of treatment of DCMs for an optimal mean palladium grain size can be established in a special study and was beyond the focus of the present work.

The treatment conditions, composition, and specific surface areas of the starting powders and compacts are listed in the table.

The fact that the specific surface area of the material increases after pressuring is explained by partial disintegration of the powder and formation of smaller particles. Figure 5 shows images of annealed and pressed Pd/Al_2O_3 material.

Comparison of the bright- and dark-field images of the particles studied with their electron diffraction patterns suggests that the main part of palladium grains in the Pd/Al_2O_3 catalysts was smaller than 10 nm.

The catalytic activity of the samples was estimated in the oxidation of hydrogen with atmospheric oxygen. Note that catalytic hydrogen oxidation is a practically important process: the catalytic flameless oxidation of hydrogen makes it possible to solve the problem of providing safety of nuclear reactors. Dispersed platinum metals deposited on an inert support are most commonly used as the catalysts [84].

The inhibitory effect of water is a serious problem in this reaction. Vlasov et al. [85] compared the activities of Pd/γ-Al_2O_3 and Pt/γ-Al_2O_3 catalysts with different porous structures. Increasing content of water vapors increased the characteristic temperature of hydrogen oxidation with the participation of the studied catalysts. This effect was most pronounced with fine-pored samples, where the probability of

capillary condensation of water vapors inhibiting the catalytic process was quite high. A conclusion was thus drawn that substrates with a low specific surface area are the most suitable. Note that in the hydrogen recombiners at nuclear power plants are equipped with special heaters for hydrogen-containing mixtures, which is necessary in view of the fact that the inhibitory effect of capillary condensation is especially strong at low temperatures. To reduce the effect of capillary condensation of water vapors is of interest in the context of the problem of fuel cell improvement. In this case, the inhibitory effect of water was reduced due to the use of hydrophobic catalysts [86, 87].

As found in [87–89], the palladium catalyst exhibited high efficiency and economic feasibility in hydrogen oxidation, but multiday measurements revealed decreasing activity of this catalyst. The strong binding of the active substance and substrate, provided by the dusty plasma technology, may favor enhanced stability of the catalyst.

The catalytic activity study was performed in a flow-type quartz reactor with a fixed-bed catalyst at atmospheric pressure; catalyst load 0.1 ± 0.01 g. Gases (air and hydrogen) were mixed directly before they were let into the reactor. The initial concentration of hydrogen was varied in the range 1–8.4%. The flow rate of the air–hydrogen mixture was 50 cm^3/min. The hydrogen concentration at the reactor outlet was measured on line with a selective calibrated electrochemical sensor. The reference was sample 5K (see table) which is a catalyst obtained by impregnation of a high-porous substrate (γ-Al_2O_3) and containing ~1 at % Pd.

In the presence of catalysts 3 and 4 (see table), unlike what was observed with the other catalysts studied, the reaction initiated without external heating at the hydrogen concentration 4%. As the initial concentration of hydrogen was decreased, the reaction in the presence of catalysts 3 and 4 occurred without external heating up to the lowest studied hydrogen concentration of 1%. With the other catalysts, the conversion of hydrogen decreased to zero within a few minutes, when the initial hydrogen concentration was decreased to 1–2%.

In sample 4 (Pd/ ZrO_2), the dispersity of palladium is sufficiently high at a low specific surface area of the substrate. The reaction occurs exclusively at the outer surface of catalyst particles, from which water is much more efficiently blown away by the gas flow than in the reaction of the reference catalyst 5K having a high specific surface area. In the latter case, the reaction occurs inside pores; therewith, a large quantity of water is formed, and at a low temperature it is almost not released from pores and prevents access of reagents to the active centers of the catalyst surface.

Apparently, the annealing temperature 870°C is close to optimal both for complete decomposition of the aluminide and for release of palladium metal with required dispersion characteristics in sample 3 (Pd/α-Al_2O_3). Note that this temperature is much higher than the sintering temperature of palladium grains deposited by traditional methods in the surface of the oxide substrate (641°C). However, at a higher annealing temperature (1000°C) the process of association of palladium grains is probably initiated in the catalysts with combined coatings, as evidenced by the decreased activity of sample 2. The low activity of sample 1 can be explained by a low annealing temperature (650°C) insufficient for complete decomposition of palladium aluminide and release of active grains.

Superhard Material

The most widespread industrial technology for the production of diamond compacts and double-layer plates (a diamond layer on a WC–Co alloy substrate) involves high-pressure sintering of diamond in the presence of a cobalt activating additive (binder). Cobalt functions as solvent for carbon and as a catalyst for the graphite–diamond conversion, thereby favoring diamond sintering and formation of a rigid diamond framework [3, 6, 90–92]. However, the difference in the thermal expansion coefficients of the matrix and inclusions leads to cracking of the diamond material and, as a result, rapid wear of instrument. The smaller is the size of cobalt inclusions and the total content of cobalt in diamond compacts, the higher is the thermal stability of the material. The cobalt content in commercial compacts is usually no less than 5–10 vol % [2].

A process for the production from a diamond powder of a diamond ceramics with a low binder concentration was developed [32, 92]. A uniform cobalt coating on 3–7-μm diamond particles confined as a fine dispersion in plasma was prepared by magnetron sputtering (Fig. 6) [92]. The cobalt concentration in the diamond powder is 2–3 wt %.

Oxidation of the cobalt coating with atmospheric oxygen may deteriorate the sintering capacity of the powder. Thermodynamic analysis of the Co–C–O system showed that cobalt oxide can be reduced by

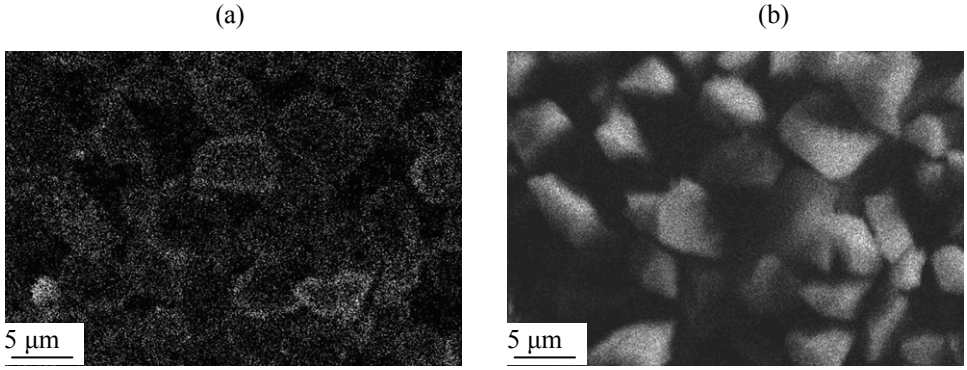

Fig. 6. Images of cobalt-coated diamond powder particles, obtained with (a) cobalt and (b) carbon characteristic X-ray radiation.

annealing at 700°C. A procedure of reducing annealing of a cobalt-coated diamond powder in pure argon in a reaction vessel before sintering was developed. Finely grained diamond compacts with low cobalt contents were obtained at a pressure of 8 GPa and a temperature of 1700–1800°C. The described treatment sequence allows production of compacts with high ultrasound velocities and elastic moduli [92].

Material with a Low Friction Coefficient

A new class of materials–quasicrystals–feature an unusual combination of properties, specifically, a low friction coefficient, high wear resistance, high corrosion resistance, and low adhesion [93, 94]. Materials with such properties may be in demand in modern technics. However, quasicrystalline materials are too brittle to be used per se. The task to create a composite material having as low friction coefficient as quasicrystals but much more plastic can be solved by introducing a metal binder into a quasicrystal powder and its subsequent compacting.

Dusty plasma deposition was used to produce disperse composite materials comprising Al–Cu–Fe quasicrystal powders comprising particles with nickel nanoshells [95]. These powders were subjected to cold compaction followed by sintering in hydrogen to obtain macrocomposites. At 750°C, strong materials which were not destroyed during tribological testing formed. Even though these samples contain about 50% of the crystalline β-phase, their measured friction coefficients proved to be close to the friction coefficient of the Al-Cu-Fe quasicrystal.

CONCLUSIONS

Plasma methods of surface modification of micron- and submicron-size powder particles can be used in solving problems of powder metallurgy, developing supported catalysts, and producing composite ceramics. The methods involving confinement of a cloud of levitating dust particles in plasma and magnetron sputtering of materials is quite efficient in such applications. Prolonged confinement of particles in a large-volume cloud in a characteristic range of low gas pressures can be used for magnetron sputter deposition of coatings on particles. In the realization of the proposed process scheme, we took into account the possibility of particle agglomeration in the cloud and the effect of the plasma generated by a magnetron sputter on the dust cloud.

It was shown that the developed process is efficient in producing disperse composite materials in a micron particle size, with a uniform coating up to a few tens of nanometers in thickness.

These powders can be used to produce materials with improved characteristics.

ACKNOWLEDGMENTS

The work was financially supported in part by RFBR grant no. 13-02-01161 and ROSATOM project no. N.4h.44.90.13.1107.

REFERENCES

1. Travitzky, N., *Adv. Appl. Ceram*., 2012, vol. 111, no. 5, pp. 286–300.
2. Akaishi, M., Ohsawa, T., and Yamaoka, S., *J. Am. Ceram. Soc*., 1991, vol. 74, pp. 5–10.
3. Katzman, H. and Libby, W.F., *Science*, 1971, vol. 172, pp. 1132–1133.
4. Akaishi, M., Yamaoka, S., Tanaka, J., Ohsawa, T., and Fakunaga, O., *J. Am. Ceram. Soc*., 1987, vol. 70, pp. 237–239.
5. Hong, S.-M., Akaishi, M., Kanda, H., and Osawa, T.,

J. Mater. Sci. Lett., 1988, vol. 23, pp. 3821–3826.

6. Shige, T., Endo, S., Fujita, E.F., Tomii, Y., *Science and Technology of New Diamond*, Saito, S., Fakunaga, O., and Yoshikava, M., Eds., Tokyo: Terra Scientific, 1990, pp. 251–255.
7. Wang, B., Ji, Z., Zimone, F.T., Janowski, G.M., and Rigsbee, J.M., *Surf. Coat. Tech*., 1997, vol. 91, nos. 1–2, pp. 64–68.
8. Haraguchi, M., Komatsu, F., Tajiri, K., Okamoto, T., Fukui, M., and Kato, S., *Surf. Sci*., 2004, vol. 548, nos. 1–3, pp. 59–66.
9. Bismarck, A., Lee, A.F., Sarac, A.S., and Wilson, K., *Comp. Sci. Tech*., 2005, vol. 65, pp. 1564–1573.
10. Chujiang, C., Xiaozheng, Y., Zhigang, S., and Yushan, X., *J. Phys. D: Appl. Phys*., 2007, vol. 40, pp. 6023–6026.
11. Mangeney, C., Qin, Z., Dahoumane, S.A., Adenier, A., Herbst, F., Boudou, J.-P., Pinson, J., and Chehimi, M.M., *Diamond Relat. Mater*., 2008, vol. 17, no. 11, pp. 1881–1887.
12. Khabashesku, V.N., Margrave, J.L., and Barrera, E.V., *Diamond Relat. Mater*., 2005, vol. 14, nos. 3–7, pp. 859–866.
13. Wang, H.-D., Yang, Q., and Niu, C.H., *Diamond Relat. Mater.*, 2010, vol. 19, nos. 5–6, pp. 441–444.
14. Emig, G., Popovska, N., Schoch, G., and Stumm, T., *Carbon,* 1998, vol. 36, no. 4, pp. 407–415.
15. Varadarajan, S., Pattanaik, A.K., and Sarin, V.K., *Surf. Coat. Tech*., 2001, vol. 139, nos. 2–3, pp. 153–160.
16. Czok, G. and Werther, J., *China Particuol*., 2005, vol. 3, nos. 1–2, pp. 105–112.
17. Caussat, B. and Vahlas, C., *Chem. Vapor Depos*., 2007, vol. 13, no. 9, pp. 443–445.
18. Arai, T., Fujita, H., Watanabe, M., and Diego, S., *Thin Solid Films*, 1987, vol. 154, pp. 387–401.
19. Shin, H.S. and Goodwin, D.G., *Mater. Lett*., 1994, vol. 19, April, pp. 119–122.
20. Bi, H., Jiang, P., Jean, R.-H., and Fan, L.-S., *Chem. Eng. Sci*., 1992, vol. 47, no. 12, pp. 3113–3124.
21. Danilin, B.S., *Primenenie nizkotemperaturnoi plazmy dlya naneseniya tonkikh plenok* (Application of Low-Temperature Plasma for Deposition of Thin Films), Moscow: Energoatomizdat, 1989.
22. Zhiglinskiy, A.G. and Kuchinskiy, V.V., *Massoperenos pri vzaimodeistvii plazmy s poverkhnost'yu* (Mass Transfer in the Plasma–Surface Interaction), Moscow: Energoatomizdat, 1991.
23. Dostanko, A.P. and Grushetskii, S.V., *Plazmennaya metallizatsiya v vakuume* (Plasma Metallization in a *Vacuum*), Minsk: Nauka i Tekhnika, 1983.
24. Schwarz, B., Schrank, C., Eisenmenger-Sittner, C., Stöger-Pollach, M., Rosner, M., and Neubauer, E., *Surf. Coat. Tech*., 2006, vol. 200, nos. 16–17, pp. 4891–4896.
25. Poelman, H., Eufinger, K., Depla, D., Poelman, D., De Gryse, R., Sels, B.F., and Marin, G.B., *Appl. Catal. A: General*, 2007, vol. 325, no. 2, pp. 213–219.
26. Chan, K.-Y., Luo, P.-Q., Zhou, Z.-B., Tou, T.-Y., and Teo, B.-S., App. *Surf. Sci*., 2009, vol. 225, no. 10, pp. 5186–5190.
27. Yu, X., Xu, Z., and Shen, Z., *J. Phys. D: Appl. Phys*., 2007, vol. 40, no. 9, 2894–2898.
28. Wasa, K., Kitabatake, M., and Adachi, H., *Thin Film Materials Technology: Sputtering of Compound Materials*, Norwich, NY: William Andrew, 2004.
29. Vysikailo, F.I., Mitin, V.S., and Mitin, A.V., *Nanotekhnika*, 2010, no. 4, issue 24, pp. 10–22.
30. Mankelevich, Yu.A., Mitin, A.V., Mitin, V.S., Pal', A.F., Rakhimova, T.V., Ryabinkin, A.N., Serov, A.O., and Luchkin, S.Yu., *Tech. Phys. Lett*., 2013, vol. 39, p. 39.
31. Ivanov, A.S., Mitin, V.S., Pal', A.F., Ryabinkin, A.N., Serov, A.O., Skryleva, E.A., Starostin, A.N., Fortov, V.E., and Shul'ga, Yu.M., *Doklady Physics*, 2004, vol. 49, no. 3, pp. 163–166.
32. Ekimov, E.A., Ivanov, A.S., Pal', A.F., Ryabinkin, A.N., Serov, A.O., Starostin, A.N., Fortov, V.E., Sadykov, R.A., Mel'nik, N.N., and Presh, A., *Doklady Physics*, 2005, vol. 50, no. 7, pp. 351–354.
33. Belov, I.A., Ivanov, A.S., Ryabinkin, A.N., and Serov, A.O., *Entsiklopediya nizkotemperaturnoi plazmy* (Encyclopaedia of Low-Temperature Plasma), 2006, vol. 1.
34. Hell, J., Horkel, M., Neubauer, E., and Eisenmenger-Sittner, C., *Vacuum*, 2009, vol. 84, no. 4, pp. 453–457.
35. Hell, J., Chirtoc, M., Eisenmenger-Sittner, C., Hutter, H., Kornfeind, N., Kijamnajsuk, P., Kitzmantel, M., Neubauer, E., and Zellhofer, K., *Surf. Coat. Technol*., 2012, vol. 208, pp. 24–31.
36. Lowe, A. and Hosford, C., *J. Vac. Sci. Technol*., 1979, vol. 16, no. 2, pp. 197–199.
37. Yu, X. and Shen, Z., *J. Magn. Magn. Mater*., 2009, vol. 321, no. 18, pp. 2890–2895.
38. Yu, X. and Shen, Z., *Vacuum*, 2011, vol. 85, no. 11, pp. 1026–1031.
39. Cairns, J.A., Nelson, R.S., and Barnfield, R.W., US Patent 4046712, 1977.
40. Haas, V. and Birringer, R., *Nanostruct. Mater*., 1992, vol. 1, pp. 491–504.
41. Takeuchi, A. and Wise, H., *J. Catal*., 1983, vol. 83, no. 2, pp. 477–479.
42. Albers, P., Seibold, K., Mcevoy, A.J., and Kiwi, J., *J. Phys. Chem*., 1989, vol. 93, no. 4, pp. 1510–1515.
43. Fedotov, A.A., Grigoriev, S.A., Lyutikova, E.K., Millet, P., and Fateev, V.N., *Int. J. Hydrogen Energy*, 2012, pp. 7–11.
44. Veith, G.M., Lupini, A.R., Pennycook, S.J., Ownby, G.W., and Dudney, N.J., *J. Catal*., 2005, vol. 231, no. 1,

pp. 151–158.
45. Gavrikov, A.V., Dorokhov, V.G., Ivanov, A.S., Pal', A.F., Petrov, O.F., Ryabinkin, A.N., Savchenko, V.I., Serov, A.O., Skryleva, E.A., and Starostin, A.N., *Doklady Physics*, 2010, vol. 55, no. 2, pp. 55–57.
46. Yu, X. and Shen, Z., *Powder Technol*., 2008, vol. 187, no. 3, pp. 239–243.
47. Schmid, G., Eisenmenger-Sittner, C., Hell, J., Horkel, M., Keding, M., and Mahr, H., *Surf. Coat. Technol*., 2010, vol. 205, no. 7, pp. 1929–1936.
48. Baechle, D.M., Demaree, J.D., Hirvonen, J.K., and Wetzel, E.D., *Surf. Coat. Technol*., 2013, vol. 221, pp. 94–103.
49. Geldart, D. and Abrahamsen, A.R., *Powder Technol*., 1978, vol. 19, no. 1, pp. 133–136.
50. Chen, G., Chen, S., Zhou, M., Feng, W., Gu, W., and Yang, S., *J. Phys. D: Appl. Phys*., 2006, vol. 39, no. 24, pp. 5211–5215.
51. Snyder, H.R., Currier, R.P., and Murillo, M.S., *Appl. Phys. Lett*., 2000, vol. 76, no. 18, pp. 2511–2513.
52. Kersten, H., Schmetz, P., and Kroesen, G.M.W., *Surf. Coat. Technol*., 1998, vols. 108–109, nos. 1–3, pp. 507–512.
53. Stoffels, E., Stoffels,W.W., Kersten, H., Swinkels, G., and Kroesen, G.M.W., *Phys. Scr*., 2001, vol. 89, pp. 168–172.
54. Ivanov, A., Mitin, V., Pal, A., Ryabinkin, A., Serov, A., Skryleva, E., Starostin, A., Fortov, V., Shulga, Y., *Plasma Processes and Polymers*, d'Agostino, R., Favia, P., Oehr, C., and Wertheimer, M., Eds., Weinheim: Wiley–VCH, 2005, pp. 455–464.
55. Rudavets, A.G., Ryabinkin, A.N., and Serov, A.O., *Plasma Proc. Polym*., 2011, vol. 8, no. 4, pp. 346–352.
56. Belov, I.A., Ivanov, A.S., Pal, A.F., Ryabinkin, A.N., and Serov, A.O., *Phys. Lett. A*, 2002, vol. 306, pp. 52–56.
57. Mankelevich, Yu.A., Olevanov, M.A., Pal', A.F., Rakhimova, T.V., Ryabinkin, A.N., Serov, A.O., and Filippov, A.V., *Plasma Phys. Reports*, 2009, vol. 35, pp. 191–199.
58. Belov, I.A., Ivanov, A.S., Ivanov, D.A., Pal', A.F., Starostin, A.N., Filippov, A.V., Dem'yanov, A.V., and Petrushevich, Yu.V., *J. Exp. Theor. Phys.*, 2000, vol. 90, no. 1, p. 93.
59. Filippov, A.V., Zagorodnii, A.G., Momot, A.I., Pal', A.F., and Starostin, A.N., *J. Exp. Theor. Phys.*, 2007, vol. 105, no. 4, p. 831.
60. Pal, A.F., Ryabinkin, A.N., and Serov, A.O., *Proc. VII Int. Conf. Plasma Physics and Plasma Technology*, Minsk, 2012, pp. 805–807.
61. Pal', A.F., Ryabinkin, A.N., Serov, A.O., Dyatko, N.A., Starostin, A.N., and Filippov, A.V., *JETP*, 2012, vol. 114, p. 535.
62. Bohren, C.F. and Huffman, D.R., *Absorption and Scattering of Light by Small Particles*, Wiley-VCH, 1998. p. 544.
63. Huang, F.Y. and Kushner, M.J., *J. Appl. Phys*., 1997, vol. 81, no. 9, pp. 5960–5965.
64. Lapenta, G., *Phys. Scr*., 2001, vol. 599, pp. 599–604.
65. Olevanov, M.A., Mankelevich, Yu.A., and Rakhimova, T.V., *J. Exp. Theor. Phys.,* 2004*,* vol. 98, no. 2, p. 287.
66. Stevens, M.J. and Robbins, M.O., *J. Chem. Phys*., 1993, vol. 98, no. 3, pp. 2319–2324.
67. Window, B. and Savvides, N., *J. Vac. Sci. Technol*. A, 1986, vol. 4, no. 2, pp. 196–202.
68. Kashtanov, P.V., Smirnov, B.M., and Hippler, R., *Phys. Usp.,* 2007, vol. 50, p. 455.
69. Somekh, R.E., *J. Vac. Sci. Technol*. A, 1984, vol. 2, pp. 1285 – 1291.
70. Augustyniak, E., Filimonov, S., and Lu, C., *Proc. SPIE Conf. on Process, Equipment, and Materials Control in Integrated Circuit Manufacturing IV*, Santa Clara, CA, 1998, pp. 192–200.
71. Turner, G.M., Falconer, I.S., James, B.W., and McKenzie, D.R., *J. Appl. Phys*., 1989, vol. 65, pp. 3671–3679.
72. Kolev, I. and Bogaerts, A*., IEEE Trans. Plasma Sci*., 2006, vol. 34, no. 3, pp. 886–894.
73. Costin, C., Marques, L., Popa, G., and Gousset, G., *Plasma Sources Sci. Technol*., 2005, vol. 14, no. 1, pp. 168–176.
74. Costin, C., Minea, T., Popa, G., and Gousset, G., *Plasma Process. Polym*., 2007, vol. 4, pp. S960–S964.
75. Flanagan, T.M. and Goree, J., *Phys. Plasmas*, 2006, vol. 13, issue 12, pp. 123504–123504–11.
76. Pal, A.F., Ryabinkin, A.N., Serov, A.O., Dyatko, N.A., Starostin, A.N., and Filippov, A.V., *J. Exp. Theor. Phys*., 2012, vol. 114, 3, pp. 535–546.
77. Rossnagel, S.M. and Kaufman, H.R., *J. Vac. Sci. Technol*. A, 1987, vol. 5, no. 1, pp. 88–91.
78. Maurer, H.R., Basner, R., and Kersten, H., *Contrib. Plasma Phys*., 2010, vol. 50, no. 10, pp. 954–961.
79. Hoffman, D.W., *J. Vac. Sci. Technol*. A, 1985, vol. 3, pp. 561–566.
80. Benilov, M.S., *Plasma Sources Sci. Technol*., 2009, vol. 18, p. 1.
81. Gurrappa, I. and Wilson, A., K.D.P., *J. Coat. Technol. Res*., 2009, vol. 6, no. 2, pp. 257–268.
82. Muller, C.A., Maciejewski, M., Koeppel, R.A., and Baiker, A., *J. Catal.,* 1997, vol. 43, no. 3 pp. 6–43.
83. Ekimov, E.A., Sadykov, R.A., Gierlotka, S., Presz, A., Tatyanin, E.V., Slesarev, V.N., and Kuzin, N.N., *Instruments and Experimental Techniques*, 2004, vol. 47, pp. 276–278.
84. Bekman, I.N., *Yadernaya industriya: Kurs lektsii* (Nuclear Industry: A Series of Lectures) Moscow: Mosk. Gos. Univ., 2005.

85. Vlasov, E.A., Gusarov, V.V., Postnov, A.Yu., and Mal'tseva, N.V., *Trudy 4 Rossiiskoi konferentsii "Fizicheskie problemy vodorodnoi energetiki"* (Proc. 4th Russian Conf. "Physical Problems of Hydrogen Energy"), St. Petersburg: Fiziko-Tekhnicheskii Institut im. A.F. Ioffe, Ross. Akad. Nauk, 2007, pp. 3–12.
86. Johansson, A., Försth, M., and Rosén, A., *Surf. Sci*., 2003, vol. 529, nos. 1–2, pp. 247–266.
87. Sakharovskiy, Yu.A., Shkurenok, D.Yu., and Lomazov, A.V., *Khim. Prom-st Segodnya*, 2009, no. 12, pp. 5–9.
88. Johansson, M. and Ekedahl, L.-G., *Appl. Surf. Sci*., 2001, vol. 180, pp. 27–35.
89. Wei, T.C. and Phillips, J., *Adv. Catal*., 1996, vol. 41, pp. 359–421.
90. Uehara, K. and Yamaya, S., *Science and Technology of New Diamond*, Saito, S., Fakunaga, O., and Yoshikava, M., Eds., Tokyo: Terra Scientific, 1990, pp. 203–209.
91. Ekimov, E.A., Suetin, N.V.,Popovich, A.F., and Ralchenko, V.G., *Diamond Relat. Mater*., 2008, vol. 17, pp. 838–843.
92. Ekimov, E.A., Borovikov, N.F., Ivanov, A.S., Leonov, A., Pal', A.F., Ryabinkin, A.N., Serov, A.O., and Starostin, A.N., *Investigated in Russia*, 2009, no. 12, pp. 562–571. http://www.sci-journal.ru/articles/2007/065.pdf.
93. *Physisal Properties of Quasicrystals*, Stadnik, Z.M., Ed., Berlin: Springer, 1999.
94. Vekilov, Yu.Kh. and Chernikov, M.A., *Phys. Usp.*, 2010, vol. 180, no. 6, pp. 561–586.
95. Ivanov, A.S., Kruglov, V.S., Pal', A.F., Ryabinkin, A.N., Serov, A.O., Shaitura, D.S., Starostin, A.N., Gavrikov, A.V., Petrov, O.F., and Fortov, V.E., *Tech. Phys. Lett*., 2011, vol. 37, no. 10, p. 917.